ELSEVIER

Journal of Nuclear Materials 288 (2001) 92–99

journal of nuclear materials

www.elsevier.nl/locate/jnucmat

A mechanism for the sintered density decrease of UO_2–Gd_2O_3 pellets under an oxidizing atmosphere

Kun Woo Song *, Keon Sik Kim, Jae Ho Yang, Ki Won Kang, Youn Ho Jung

Advanced LWR Fuel Development, Korea Atomic Energy Research Institute, P.O. Box 105, Yusong, Daejon 305-600, South Korea

Received 15 August 2000; accepted 17 November 2000

Abstract

A mixture of UO_2 and Gd_2O_3 powders was pressed into compacts and sintered under various atmospheres ranging from reducing to oxidizing gases. The sintered density of UO_2–10 wt% Gd_2O_3 pellets decreases with increasing oxygen potential of the sintering atmosphere. Dilatometry and X-ray diffraction studies indicate that the delay of densification takes place between 1300°C and 1500°C, along with the formation of (U,Gd) O_2. A very large solubility of Gd_2O_3 in UO_2 relative to the reverse solubility might cause Gd ions to diffuse into UO_2 so directionally that new pores are produced at the places of Gd_2O_3 particles. The new pores may be difficult to shrink and thus lead to the density decrease under an oxidizing atmosphere but not under a reducing atmosphere, because a driving force for the shrinkage of new pores may be smaller under an oxidizing atmosphere than under a reducing atmosphere. © 2001 Elsevier Science B.V. All rights reserved.

1. Introduction

UO_2–Gd_2O_3 fuel pellets are widely used as a burnable absorber to suppress initial excess reactivity at the begin of life (BOL) in LWRs. The fabrication method of UO_2–Gd_2O_3 pellets has been developed based mainly on that of UO_2 fuel pellets [1,2], and thus it includes the processes of mixing or milling, pressing and sintering as the fabrication method of UO_2 fuel pellets does. However, UO_2–Gd_2O_3 pellets are more difficult to produce than UO_2 pellets because the UO_2–Gd_2O_3 pellet is apt to have a smaller grain size and an inhomogeneous Gd distribution under the same sintering temperature and atmosphere.

The fabrication method of UO_2–Gd_2O_3 pellets has been widely studied in order to improve the fuel properties. The effect of powder properties on the sintered density, grain size and Gd homogeneity of UO_2–Gd_2O_3 pellets has been investigated [3,4]. Riella et al. [4] showed that co-precipitated $(U,Gd)O_2$ powder was better in getting a homogeneous Gd distribution than any other powder. The effect of sintering atmosphere on the properties of UO_2–Gd_2O_3 pellets has been studied by some workers [5–7]. The published literature reported that the sintered density decreases as the oxygen potential of the sintering atmosphere increases.

Regarding the density decrease under an oxidizing atmosphere, Yuda and Une [6] observed that pores were newly formed in accordance with the decrease in density, and they simply explained that the sintering process between UO_2 and UO_2 particles rapidly progressed under an oxidizing atmosphere prior to that between UO_2 and Gd_2O_3 particles, so that new pores formed just near the Gd_2O_3 particles by the shrinkage of surrounding UO_2 particles. A more detailed study on the pore formation has not been carried out until now.

The purpose of this work is to understand the effect of the oxygen potential of the sintering atmosphere on the sintering behavior of UO_2–Gd_2O_3 pellets. The density decrease, $(U,Gd)O_2$ formation and changes in microstructure are investigated under various sintering atmospheres. A mechanism for the density decrease is proposed and discussed.

2. Experimental

A powder mixture of UO_2 and Gd_2O_3 was prepared as starting material for the pellet fabrication. The UO_2

---

* Corresponding author: Tel.: +82-42 868 2579; fax : +82-42 868 2403.

E-mail address: kwsong@kaeri.re.kr (K.W. Song).

PII: S0022-3115(00)00721-2

powder used was made through the ammonium uranyl carbonate (AUC) process [8]. The UO_2 powder had a round shape and a BET surface of 5 m^2/g. The average particle sizes of the UO_2 and Gd_2O_3 powders, which were measured by the laser light scattering method, were 17 and 4.1 μm, respectively. The UO_2 and Gd_2O_3 powders were mixed in a tumbling mixer for 2 h to form a uniform powder mixture with the composition UO_2–10 wt% Gd_2O_3. Three independent samples for chemical analysis were taken and analyzed after mixing. The results showed that the difference between the three gadolinium contents was less than 0.2 wt%.

The powder mixture was pressed into compacts (green pellets), which had a density of 6.0 g/cm^3. The compacts were heated at 1680°C at 5°C/min and then held for 4 h to sinter to UO_2–10 wt% Gd_2O_3 pellets. Four sintering gas atmospheres with different oxygen potentials were used: hydrogen (H_2) and three gas mixtures of hydrogen and carbon dioxide (CO_2). The hydrogen gas used in this work had a dew point of −30°C and thus contained a water vapor of 5×10^{-2} vol.% as an impurity. The CO_2-to-H_2 volume ratios in the CO_2/H_2 gas mixtures were 0.05, 0.15, and 0.30.

The gas mixture of H_2 and CO_2 reacts in thermodynamic equilibrium at elevated temperatures as follows:

$$CO_2 + H_2 = CO + H_2O,$$
$$H_2O = H_2 + \tfrac{1}{2}O_2.$$

The resultant composition of a gas mixture is determined by the equilibrium constant, which is a function of the temperature of the gases. The SOLGASMIX program [9], which can calculate the Gibbs free energy and equilibrium constant of a reaction, was used to calculate the oxygen partial pressures of the sintering atmospheres under the total gas pressure of 1 bar. The calculated results are plotted against temperature in Fig. 1. The oxygen potential ($\Delta\bar{G}(O_2) = RT \ln p(O_2)$) increases with the CO_2-to-H_2 volume ratio. It is assumed that the oxygen potential of the pellet material changes almost in accordance with the calculated value during the heating stage of sintering, and that it is equivalent to the calculated value for the holding period at the sintering temperature. The density of the sintered pellets was determined by the water immersion method. The theoretical density (TD) of a UO_2–10 wt% Gd_2O_3 pellet was calculated to be 10.56 g/cm^3 using the following relation [1]: TD(g/cm^3) = 10.96–0.04 wt% of Gd_2O_3. Sintered pellets were sectioned longitudinally and polished, and the microstructure was observed.

In order to study the dependence of densification on temperature, the shrinkage of compacts was measured in an axial direction with a linear variable differential transformer (LVDT) transducer in a push-rod type dilatometer. UO_2–10 wt% Gd_2O_3 and UO_2 compacts were heated to 1650°C at a rate of 5°C/min under reducing and oxidizing atmospheres: the reducing one was hydrogen gas with a water vapor of 5×10^{-2} vol.%, and the oxidizing one was a gas mixture of CO_2 and CO, in which the CO_2-to-CO volume ratio was 0.15. The oxygen potential of this CO_2/CO gas mixture is similar to that of the CO_2/H_2 gas mixture having a CO_2-to-H_2 volume ratio of 0.30 above about 1000°C (see Fig. 1). The CO_2/CO gas mixture was used in place of the CO_2/H_2 gas mixture to avoid the damage of Pt thermocouple in a dilatometer.

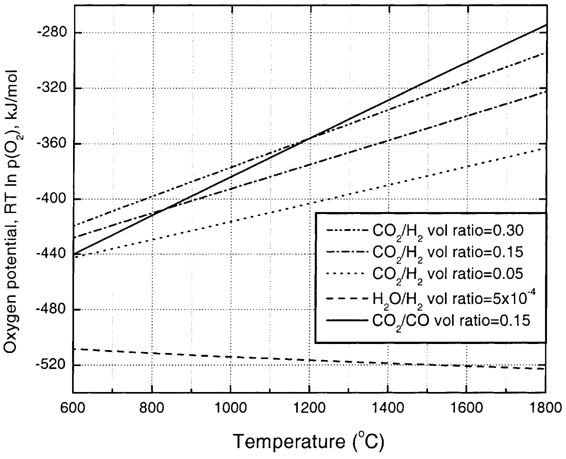

Fig. 1. Oxygen potentials of various sintering gases as a function of temperature.

Partly sintered pellets were prepared by heating the compacts up to 1400°C and 1600°C in the same sintering atmospheres as the dilatometry study used. X-ray diffraction patterns were obtained from the partly sintered pellets using monochromatic Cu K_α radiation. The distribution of gadolinium concentration in the partly sintered pellets was analyzed by electron probe microanalysis (EPMA) using wavelength-dispersive X-ray spectroscopy.

3. Results

Fig. 2 shows the dependence of the sintered density of UO_2–10 wt% Gd_2O_3 pellets on the CO_2-to-H_2 volume ratio in the sintering atmospheres. The sintered density of UO_2–10 wt% Gd_2O_3 pellets is relatively low due to the low sintering temperature. The sintered density appears to increase slightly in the atmosphere with the gas ratio of 0.05, and thereafter it decreases gradually with increasing the gas ratio. The overall amount of the density decrease reaches about 2.5% TD at a gas ratio of 0.3. The density decrease of the UO_2–Gd_2O_3 pellets was found under oxidizing atmospheres also by other workers [6,10]. Yuda and Une [6] observed that the

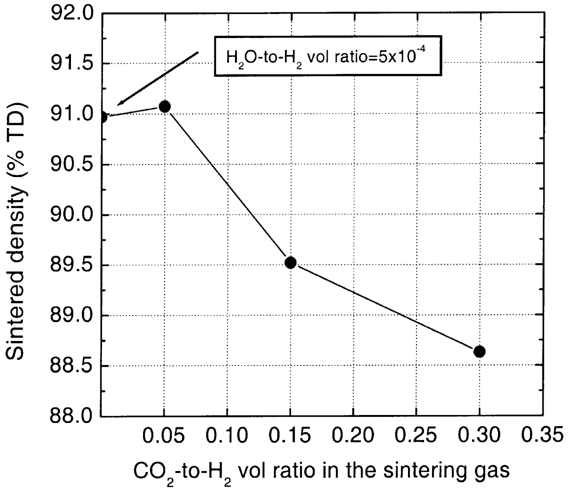

Fig. 2. Dependence of the sintered density of UO_2–10 wt% Gd_2O_3 pellets on the CO_2-to-H_2 vol ratio in the sintering atmospheres.

density began to decrease above a threshold oxygen potential. Fig. 2 indicates that the sintered density of UO_2–10 wt% Gd_2O_3 pellets begins to decrease at a CO_2-to-H_2 volume ratio between 0.05 and 0.15 and between −370 and −330 kJ/mol at 1680°C (see Fig. 1).

Figs. 3(a)–(d) show the microstructures of UO_2–10 wt% Gd_2O_3 pellets sintered in the four gas atmospheres. The number of pores appears to increase significantly with the oxygen potential (the CO_2-to-H_2 volume ratio), and the decrease in density can be attributed to the formation of new pores. An EPMA examination of the Gd concentration revealed [7] that the new pores were preferentially produced in the regions of a relatively high Gd concentration.

Figs. 4(a) and (b) show the variations in shrinkage (densification) of UO_2–10 wt% Gd_2O_3 compacts with temperature in hydrogen gas and in the CO_2/CO gas mixture. For comparison the shrinkage of UO_2 powder compacts is shown together with them. All the compacts start to densify at about 800°C, but each compact densifies quite differently over the whole temperature range. Under a reducing atmosphere (hydrogen gas), the densification of the UO_2–Gd_2O_3 compact progresses more slowly than that of the UO_2 compact, and the difference in densification between the former and the latter increases gradually in the temperature range 1000–1300°C. That difference is largest in the temperature range 1300–1500°C because the densification of UO_2–Gd_2O_3 compacts is remarkably delayed. The densification of UO_2–Gd_2O_3 compacts starts again above 1500°C.

Fig. 4(a) also shows that the densification of the UO_2–Gd_2O_3 compact under an oxidizing atmosphere (CO_2/CO gas mixture) progresses to a lesser extent than that of the UO_2 compact. The delay of densification under an oxidizing atmosphere is found in nearly the same temperature range as that under a reducing

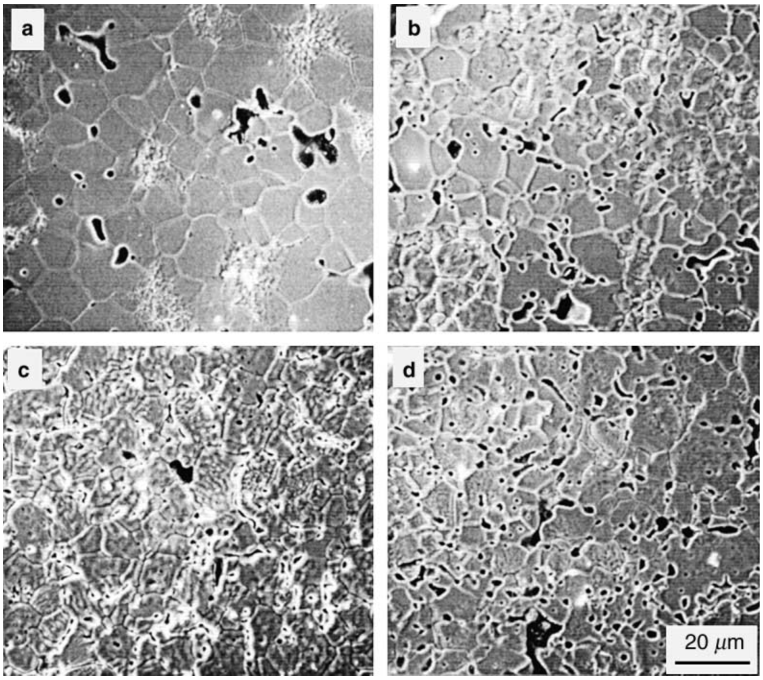

Fig. 3. Microstructures of sintered UO_2–10 wt% Gd_2O_3 pellets in various gases: (a) $H_2O/H_2 = 5 \times 10^{-4}$; (b) $CO_2/H_2 = 0.05$; (c) $CO_2/H_2 = 0.15$; (d) $CO_2/H_2 = 0.3$.

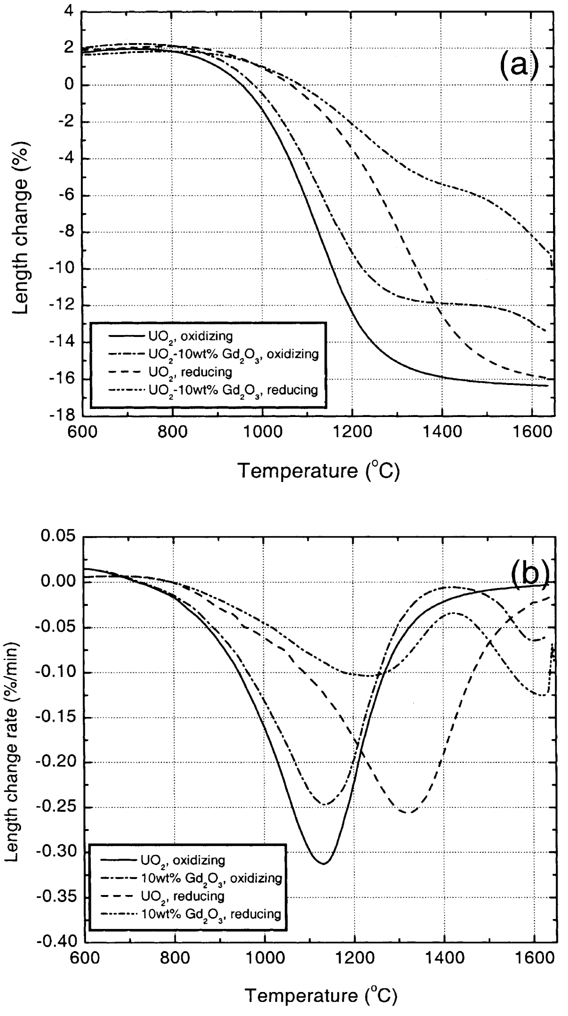

Fig. 4. Densification curves of UO_2 and UO_2–10 wt% Gd_2O_3 compacts under reducing ($H_2O/H_2 = 5 \times 10^{-4}$) and oxidizing ($CO_2/CO = 0.15$) atmospheres: (a) densification; (b) densification rate.

atmosphere. However, it takes place at a shrinkage of about 12% in length under an oxidizing atmosphere but at a shrinkage of 4–6% under a reducing atmosphere. Therefore, the delay of densification takes place in the intermediate sintering stage under a reducing atmosphere, but near the final sintering stage under an oxidizing atmosphere.

Fig. 4(a) shows that the UO_2–10 wt% Gd_2O_3 compact densifies much more under an oxidizing atmosphere than under a reducing atmosphere, but Fig. 2 shows that the sintered density is lower under an oxidizing atmosphere. This apparent disagreement can be understood by assuming that the densification of UO_2–10 wt% Gd_2O_3 compacts during the holding period at the sintering temperature progresses much more under a reducing atmosphere.

Fig. 4(b) shows the densification rates derived from the densification curves in Fig. 4(a). The UO_2 compact exhibits a single peak at 1100°C under an oxidizing atmosphere and a single peak at 1300°C under a reducing atmosphere, while the UO_2–Gd_2O_3 compact exhibits double peaks at 1100/1600°C under an oxidizing atmosphere and at 1200/1600°C under a reducing atmosphere. The UO_2–Gd_2O_3 compacts have minimum densification rates at 1400–1450°C, owing to the delay of densification. Under an oxidizing atmosphere the peak of UO_2 and the first peak of UO_2–Gd_2O_3 are very similar in temperature and rate, but under a reducing atmosphere the peak of UO_2 is much larger in rate than the first peak of UO_2–Gd_2O_3.

Fig. 5 shows the X-ray diffraction patterns of partly sintered pellets obtained at intermediate temperatures during sintering in hydrogen gas. Both the UO_2 and Gd_2O_3 phases remain up to 1200°C. At 1450°C the Gd_2O_3 phase disappears, and additionally other phases might form. Accordingly, reactions between UO_2 and Gd_2O_3 start in the temperature range of 1200–1450°C, where the densification of UO_2–Gd_2O_3 pellets is remarkably delayed (see Fig. 4(a)). Reactions between UO_2 and Gd_2O_3 initially include the formation of $(U,Gd)O_2$ and UGd_6O_{11} [11,12]. Since the UGd_6O_{11} phase is not an equilibrium phase in the composition of UO_2–10 wt% Gd_2O_3, it likely exists temporarily. So the delay of densification is mainly related to the formation of $(U,Gd)O_2$. The $(U,Gd)O_2$ phase with a strong intensity and the UO_2 phase with a weak intensity are found at 1680°C/4 h, suggesting that the $(U_{0.86}Gd_{0.14})O_2$ solid solution which corresponds to UO_2–10 wt% Gd_2O_3 in Gd content is not yet fully formed. Before the formation of $(U,Gd)O_2$, the densification could take place mainly by sintering between UO_2 and UO_2 particles. X-ray diffraction results in Fig. 5 are in good agreement with the work of Manzel and Dörr [13], who reported that the initial densification occurred mainly by sintering between UO_2 and UO_2 particles and then it was delayed by the formation of $(U,Gd)O_2$.

Fig. 6 shows the X-ray diffraction patterns of partly sintered pellets obtained at intermediate temperatures during sintering in the CO_2/CO gas mixture. Both UO_2 and Gd_2O_3 phases remain up to 1100°C, and the intensity of the Gd_2O_3 phase is slightly reduced at 1400°C. Thus reactions between UO_2 and Gd_2O_3 – mainly the formation of $(U,Gd)O_2$ – might start under an oxidizing atmosphere around 1400°C, at which the delay of densification occurs significantly. Both the $(U,Gd)O_2$ and UO_2 phases with comparable intensity are found at 1650°C/4 h, suggesting that a complete $(U_{0.86}Gd_{0.14})O_2$ solid solution has not yet been formed. Under an oxidizing atmosphere the same findings are noticed as under a reducing atmosphere; the delay of densification is related to the formation of $(U,Gd)O_2$, and the densification, which occurs before the formation of $(U,Gd)O_2$,

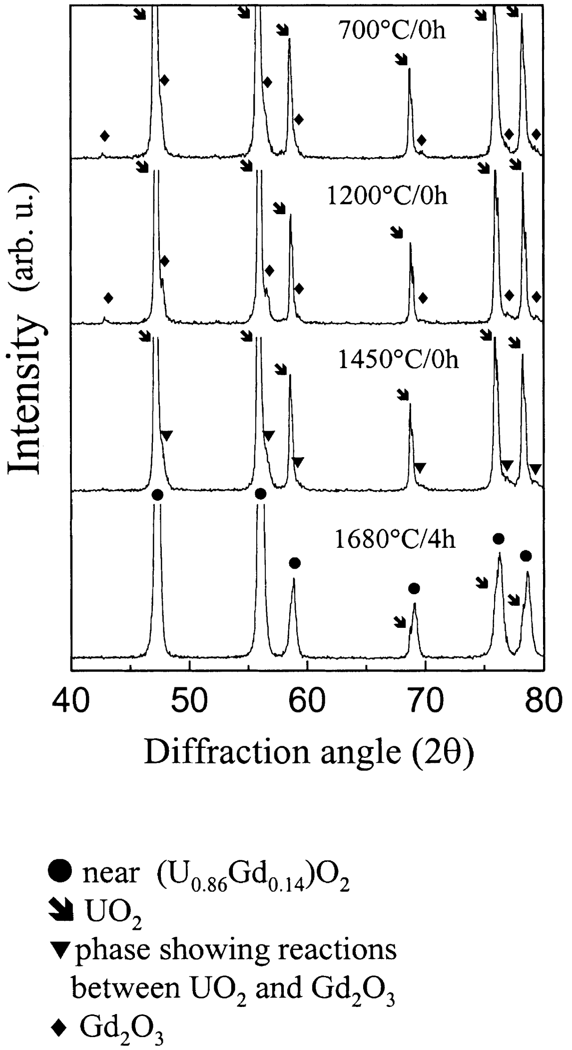

Fig. 5. X-ray diffraction patterns of partly sintered UO_2–10 wt% Gd_2O_3 pellets heated in hydrogen gas up to intermediate temperatures.

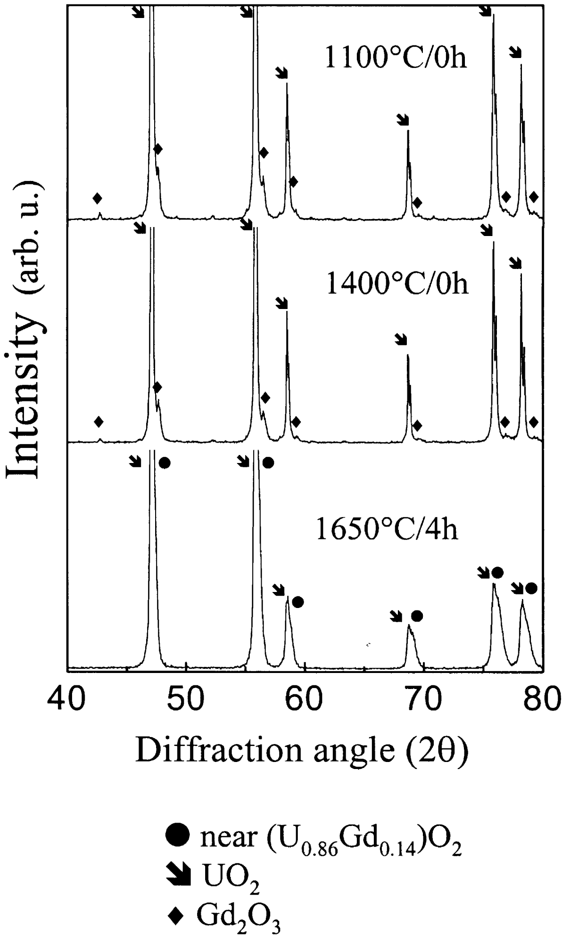

Fig. 6. X-ray diffraction patterns of partly sintered UO_2–10 wt% Gd_2O_3 pellets heated in the CO_2/CO gas mixture up to intermediate temperatures.

is mainly due to the sintering between UO_2 and UO_2 particles.

The densification curve showed that the temperature range where the delay of densification occurred was little affected by the difference in the sintering atmosphere. However, before the delay of densification, the densification through sintering between UO_2 and UO_2 particles progressed much more under an oxidizing atmosphere. Sintering between UO_2 particles can progress through the diffusion of U ions, but the formation of $(U,Gd)O_2$, which is related to the delay of densification, essentially needs the diffusion of Gd ions. It is well known [14] that the uranium diffusion in UO_2 is greatly enhanced by the increase in oxygen potential because the increased oxygen-to-uranium ratio involves oxygen interstitials and the valence of U ions changes from 4+ to 5+ or 6+. However, the diffusion of Gd ions is unlikely to be dependent on the change in oxygen potential because Gd ions have only one oxidation state of 3+. So the diffusion of Gd ions may be mainly dependent on temperature, making the formation of $(U,Gd)O_2$ at similar temperatures under oxidizing and reducing atmospheres.

Figs. 7(a) and (b) show the microstructures of UO_2–10 wt% Gd_2O_3 pellets which were heated in hydrogen up to 1400°C and 1600°C, respectively. Figs. 8(a) and (b) show the microstructures of UO_2–10 wt% Gd_2O_3 pellets which were heated in the CO_2/CO gas mixture up to 1400°C and 1600°C, respectively. Round UO_2 particles of about 20 μm can be individually distinguished in Figs. 7 and 8. The difference in pore structure between Figs. 7(b) and 8(b) suggests that the sintering of UO_2 particles progresses much more under an oxidizing atmosphere than under a reducing atmosphere. Thus a UO_2 matrix is dense in an oxidizing atmosphere but rather porous in a reducing

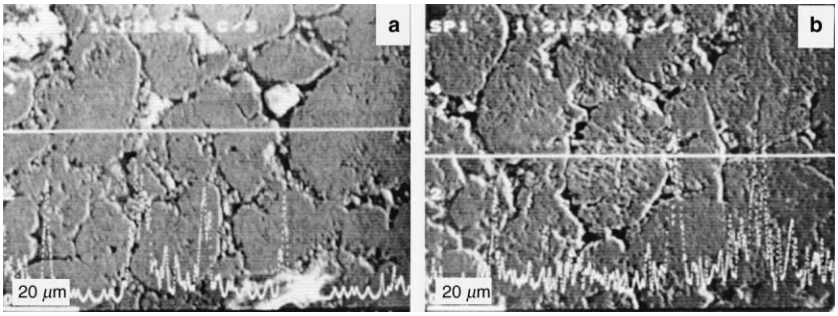

Fig. 7. SEM micrographs showing Gd concentration profile in partly sintered UO_2–10 wt% Gd_2O_3 pellets heated in hydrogen gas up to: (a) 1400°C, (b) 1600°C. (The Gd concentration is obtained along the white straight line.)

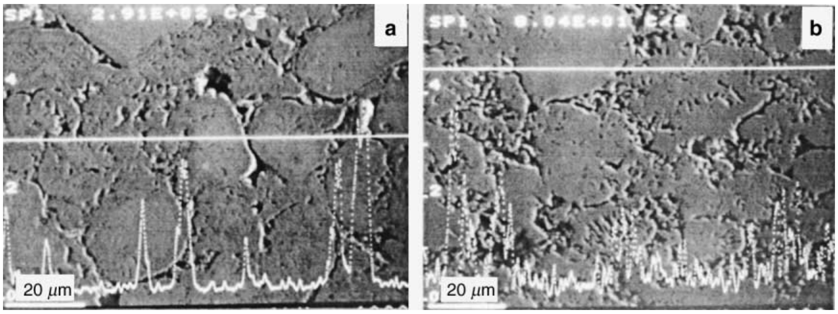

Fig. 8. SEM micrographs showing Gd concentration profile in partly sintered UO_2–10 wt% Gd_2O_3 pellets heated in the CO_2 /CO gas mixture up to: (a) 1400°C, (b) 1600°C.

atmosphere. This result can be expected from Fig. 4(a), which shows that the densification of UO_2–Gd_2O_3 pellets is much larger under an oxidizing atmosphere.

Figs. 7(a) and 8(a) show that the partly sintered pellets at 1400°C have sharp Gd concentration peaks on the interface between UO_2 and UO_2 particles. Figs. 7(b) and 8(b) show that parts of the interfaces have small and broad peaks, suggesting that the Gd ions diffuse partly into the surrounding UO_2 at 1600°C. The comparison between Fig. 7 and Fig. 8 implies that the initial dissolution behavior of Gd in UO_2 is only slightly different between reducing and oxidizing atmospheres. An interesting point is that a Gd concentration peak tends to be wide in breadth and to split into several peaks as the temperature increases.

Fig. 9 shows a set of split peaks in a region of high Gd concentration in the partly sintered pellet at 1600°C. In this region the intensity of split peaks is low at the position of pores but high between pores. This region might originally consist of Gd_2O_3 particles before sintering. It is supposed that new pores are produced during the formation of $(U,Gd)O_2$ in the region where Gd_2O_3 particles were originally placed. A similar observation was reported in UO_2–Dy_2O_3 sintering by Flipot and Delbrassine [15], who described that pores were often located in the places where Dy_2O_3 particles were situated.

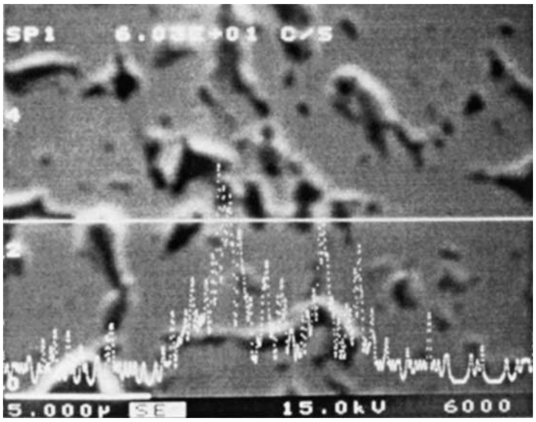

Fig. 9. SEM micrographs showing a set of the split Gd concentration peaks. (The Gd concentration is obtained along the white straight line.)

4. Discussion

According to the phase diagram of the UO_2–Gd_2O_3 system [16] that was revised from the original [11], UO_2 and Gd_2O_3 do not form a complete solid solution over the whole range of composition. The phase diagram

Table 1
Estimation of the shrinkage of new pores under reducing and oxidizing atmospheres, compared to the shrinkage of pores in a UO_2 matrix[a]

Case	Pore size	Reducing atmosphere	Oxidizing atmosphere
A	$D_p > D_d > D_{np}$	Highly shrinkable	Shrinkable
B	$D_p > D_{np} > D_d$	Shrinkable	Less shrinkable
C	$D_{np} > D_p > D_d$	Less shrinkable	Least shrinkable

[a] D_{np} is the size of new pores, D_d is the size of pores in a dense UO_2 matrix, D_p is the size of pores in a porous UO_2 matrix, D_p is assumed to be larger than D_d.

indicates that UO_2 can dissolve Gd_2O_3 up to over 20 mol% $GdO_{1.5}$, but Gd_2O_3 can dissolve UO_2 very slightly. This fact suggests that the diffusion of Gd ions into UO_2 is much more favorable in forming a (U,Gd) O_2 solid solution rather than the reverse diffusion. We found experimentally that Gd ions diffused into UO_2 but U ions did not diffuse into Gd_2O_3 when a diffusion couple of UO_2/Gd_2O_3 was annealed at 1700°C for 100 h in hydrogen gas [17]. The solubility difference between UO_2 and Gd_2O_3 and our experiment strongly suggests that Gd ions can diffuse directionally into UO_2 – at least in an initial stage of (U,Gd) O_2 formation. Such a directional flow of Gd ions might leave new pores at the original places of Gd_2O_3 particles (Kirkendall pores). In general, it is known [18] that new pores form by the Kirkendall effect when two materials that are very different in diffusivity or solubility are mixed and sintered.

The densification curve and phase analysis indicated that the delay of densification occurred together with the formation of (U,Gd)O_2 under reducing and oxidizing atmospheres. As discussed above, the formation of (U,Gd)O_2 involves the directional diffusion of Gd ions into UO_2 and the formation of new pores. Accordingly, the delay of densification can be mainly attributed to the formation of new pores during the formation of (U,Gd)O_2 under reducing and oxidizing atmospheres. It is supposed that the formation of new pores is not influenced by the oxygen potential of the sintering atmospheres since it cannot occur through the diffusion of U ions but the diffusion of Gd ions. The diffusion of Gd ions might not be dependent on the oxygen potential because Gd ions have only one oxidation state of 3+.

The directional diffusion of Gd ions into UO_2 can produce new pores very similarly under reducing and oxidizing atmospheres. After the new pores have formed, the possibility of shrinkage of the new pores might be different between the two atmospheres. The formation of new pores occurs near the final sintering stage in an oxidizing atmosphere but in the intermediate sintering stage in a reducing atmosphere (see Fig. 4(a)). The driving force for densification is generally smaller in the final sintering stage than in the intermediate sintering stage. So the further densification of new pores is likely to progress less under an oxidizing atmosphere than under a reducing atmosphere.

From the viewpoint of pore size, the shrinkage of new pores is dependent on whether they are larger than matrix pores or not. A UO_2 matrix surrounding the new pores is dense under an oxidizing atmosphere but porous under a reducing atmosphere. It is reasonable to assume that the pores in a dense UO_2 matrix are smaller in size than those in a porous UO_2 matrix. On the other hand, the new pores formed by diffusion of Gd into UO_2 are assumed to be nearly identical in size under both atmospheres. Since the driving force for pore shrinkage is inversely proportional to pore size, the difference in size between the new pores and the matrix pores plays a dominant role in the shrinkage of new pores under each atmosphere. The possibility of shrinkage of new pores is estimated under each atmosphere for every case of relative pore size, and the results are shown in Table 1.

In case A of Table 1, the new pores are expected to shrink more than the matrix pores under reducing and oxidizing atmospheres, but this expectation disagrees with the experimental results in an oxidizing atmosphere. In case C, it can be expected that the new pores shrink less than the matrix pores under both atmospheres, but this expectation is not consistent with the experimental results in a reducing atmosphere. In case B, it is expected that the new pores can shrink under a reducing atmosphere but hardly shrink under an oxidizing atmosphere, compared to the respective matrix pores. This expectation in case B is consistent with the experimental results, suggesting that the size of new pores is larger than that of matrix pores under an oxidizing atmosphere and is smaller than that of matrix pores under a reducing atmosphere. Therefore, the driving force for the shrinkage of new pores may be smaller under an oxidizing atmosphere than under a reducing atmosphere. If the new pores are much larger than the matrix pores in an oxidizing atmosphere, they will be subject to growth by absorbing vacancies from small pores in a dense matrix.

5. Conclusions

It was found that the sintered density of UO_2–10 wt% Gd_2O_3 pellets decreased and new pores formed in the region with high Gd concentration as the oxygen potential of the sintering atmosphere increased. Densification curve and phase analysis indicate that the delay of densification occurs together with the formation of $(U,Gd)O_2$ in the temperature range of 1300–1500°C under reducing and oxidizing atmospheres. Before the formation of $(U,Gd)O_2$, sintering between UO_2 and UO_2 particles takes place extensively and thus a dense UO_2 matrix is produced under an oxidizing atmosphere, but a porous UO_2 matrix is produced under a reducing atmosphere.

A mechanism for the density decrease of UO_2–Gd_2O_3 pellets can be proposed. While the formation of $(U,Gd)O_2$ progresses, new pores are produced at the original sites of Gd_2O_3 particles as a result of the directional diffusion of Gd ions into UO_2 because the solubility of Gd_2O_3 in UO_2 is much higher than the reverse solubility. The delay of densification is mainly attributed to the formation of new pores. This pore formation is likely to occur very similarly in reducing and oxidizing atmospheres, but the driving force for the densification of new pores may be different between the two atmospheres. That driving force is expected to be much smaller under an oxidizing atmosphere than under a reducing atmosphere because the new pores form near the final sintering stage under an oxidizing atmosphere, but in the intermediate sintering stage under a reducing atmosphere. In addition, the new pores might be larger in size than the surrounding UO_2 matrix pores under an oxidizing atmosphere (in a dense matrix), but might be smaller than the surrounding UO_2 matrix pores under a reducing atmosphere (in a porous matrix). Therefore, the new pores may be difficult to shrink in an oxidizing atmosphere, but may be relatively easy to shrink in a reducing atmosphere, and finally they give rise to the density decrease of sintered UO_2–Gd_2O_3 pellets under an oxidizing atmosphere.

Acknowledgements

This work has been carried out under the nuclear R&D program supported by the Ministry of Science and Technology, Korea.

References

[1] H. Assmann, J.P. Robin, in: Guidebook on Quality Control of Mixed Oxides and Gadolinium Bearing Fuels for Light Water Reactors, IAEA-TECDOC-584, IAEA, Vienna, 1983, p. 51.

[2] H. Assmann, M. Peehs, H. Roepenack, J. Nucl. Mater. 153 (1988) 115.

[3] H.H. Davis, R.A. Potter, Mater. Sci. Res. 11 (1974) 515.

[4] H.G. Riella, M. Durazzo, M. Hirata, R.A. Nogueira, J. Nucl. Mater. 178 (1991) 204.

[5] S.M. Ho, K.C. Radfod, Nucl. Technol. 73 (1986) 350.

[6] R. Yuda, K. Une, J. Nucl. Mater. 178 (1991) 195.

[7] K.W. Song, K.S. Kim, Y.S. Yoo, Y.H. Jung, J. Korean Nucl. Soc. 30 (1998) 128.

[8] C.S. Choi, J.H. Park, E.H. Kim, H.S. Shin, I.S. Chang, J. Nucl. Mater. 153 (1991) 148.

[9] HSC Chemistry for Windows, 1994, Outokump research.

[10] T. Nishida, R. Yuda, in: Advances in Pellet Technology for Improved Performance at High Burnup, IAEA-TECDOC-1036, IAEA, Vienna, 1998, p. 73.

[11] R.J. Beals, J.H. Handwerk, J. Am. Ceram. Soc. 52 (1969) 578.

[12] D. Balestrieri, Y. Philipponneau, in: Advances in Pellet Technology for Improved Performance at High Burnup, IAEA-TECDOC-1036, IAEA, Vienna, 1998, p. 63.

[13] R. Manzel, W.O. Dörr, Am. Ceram. Soc. Bull. 59 (1980) 601.

[14] H. Assmann, W.O. Dörr, M. Peehs, J. Nucl. Mater. 140 (1986) 1.

[15] A.J. Flipot, A. Delbrassine, Powder Metall. Int. 4 (1972) 134.

[16] R.S. Roth, J.R. Dennis, H.F. McMurdie, Phase Diagrams for Ceramists, vol. 3, American Ceramics Society, Westerville, OH, 1975, p. 152.

[17] J.H. Yang, K.W. Song, unpublished work.

[18] R.M. German, Sintering Theory and Practice, Wiley, New York, 1996, p. 197.